Frontiers in Superconducting Materials
(ed. A.V. Narliker, Springer-Verlag, Berlin, 2005) 683–695

PROGRESS IN Na_xCoO_2 SINGLE CRYSTAL GROWTH

D. Prabhakaran and A.T. Boothroyd

Clarendon Laboratory, Department of Physics,
University of Oxford, Parks Road, Oxford OX1 3PU, UK.

1. INTRODUCTION

The discovery of new electronic phenomena such as superconductivity, colossal magnetoresistance, and effects associated with charge and orbital, especially in cuprates, manganites, nickelates and cobaltites, has rekindled interest among the research community in layered transition metal oxides. Alkaline cobaltite (A_xCoO_2) is a good example of this trend, having been studied over a long period of time for its interesting structural, thermoelectric and transport properties [1–3]. Recently, great attention has been paid to gamma phase Na_xCoO_2, firstly because of its potential as a thermoelectric material [4], and second because of the discovery of a novel form of superconductivity in the hydrated compound ($Na_{0.3}CoO_2.1.3H_2O$) [5].

Motivated by these recent discoveries, many groups have investigated the preparation and properties of Na_xCoO_2 for a range of x. Compositions near $Na_{0.7}CoO_2$ have been of particular interest since this is the usual starting material for the synthesis of the superconducting phase [4-7]. Single phase Na_xCoO_2 can be prepared in polycrystalline form by the conventional solid-state reaction technique. Different starting materials have been used during the preparation, including oxides [1], hydroxide [8] and nitride solutions [9]. Owing to the volatile nature of sodium, a 'rapid heat-up' technique [10] has been employed, and more recently, spark plasma sintering (SPS) has also been used to achieve high density single phase material [11]. Highly textured $NaCo_2O_4$ ceramic processing has been achieved by the reactive templated grain growth method using single crystal particles [12, 13]. It is very difficult to prepare the single phase materiel with $x < 0.5$, and often Co_2O_3 or CoO will

be present in the sample as an impurity phase. Magnetic and structural properties for these impurity phases have been reported elsewhere [14-16].

The Na_xCoO_2 compound has been classified into four different phases, namely α ($0.9 \leq x \leq 1$), α' ($x=0.75$), β ($0.55 \leq x \leq 0.6$), and γ-$Na_xCo_yO_2$ ($0.55 \leq x/y \leq 0.74$), each with different cell structures, rhombohedral, monoclinic, orthorhombic and hexagonal, respectively [1]. An early neutron powder diffraction study of $Na_{0.74}CoO_2$ reported a hexagonal structure with cell parameters a=2.840 Å and c=10.811 Å, respectively, and also suggested that the Na ion can move freely between the cobalt-oxygen layers [17]. More recently, the structure of Na_xCoO_2 over a wider range of x has been studied by diffraction methods [18, 19]. Nevertheless, the c axis value of the gamma phase composition varies slightly with respect to the x concentration [10, 13, 18, 20]. Other interesting physical properties of this material are sodium ordering [21, 22] and Co^{3+}/Co^{4+} charge ordering [23, 24].

Single crystals have been grown by the flux technique using NaCl as the flux medium [4, 25-27]. Flux-grown crystals are very thin, and the maximum size reported so far is 10x10x0.1 mm^3 [25]. Recently, single crystals have also been grown by the floating-zone technique [28-31]. This method offers the possibility of preparing large crystals for experiments where size is important, such as inelastic neutron scattering. Possible difficulties of this technique are Na evaporation during the melt growth, and changes in the physical properties depending on the atmosphere used during crystal growth. These issues have not been investigated in detail before now. In this paper we describe the preparation of large Na_xCoO_2 single crystals by the floating-zone method under different conditions. We investigated the composition x = 0.75 in some detail. We report the optimum crystal growth conditions (pressure and atmosphere), phase purity and some magnetic properties of the crystals. More detailed measurements of the magnetic properties of powder and single crystal Na_xCoO_2 for a wide range of x are given in ref. [30].

2. EXPERIMENTAL METHOD

Single phase polycrystalline samples of $Na_{0.75}CoO_2$ were prepared using high-purity (>99.98%) Na_2CO_3 and Co_3O_4. The starting powders were first ground using a ball mill with acetone for homogenous mixing. The well mixed dry powder was spread on a platinum foil (instead of directly in an alumina boat to avoid reaction with Co_3O_4) and loaded into a preheated (>650°C) furnace. The use of a spread powder was found preferable to compressed pellets since the latter tended to leave an unreacted central core and hence needed more sintering. Rapid heating of the furnace to the desired maximum sintering temperature was employed to reduce the Na evaporation as reported previously [8]. To obtain single phase material, three different temperatures (850°C, 870°C and 890°C) were used for sintering the powders under oxygen flow with intermediate dry grinding. We avoided the use of solvents during the intermediate grinding since addition of acetone leads to absorption of moisture (converting unreacted Na_2O in to Na_2CO_3 and increasing the number of sintering cycles needed to obtain single phase material). All synthesized powders were analyzed carefully for Co_3O_4 and CoO impurities by powder X-ray diffraction (XRD) and magnetization measurements after each sintering process.

The feed material for the crystal growth process was prepared in the form of cylindrical rod of size 6-9 mm diameter and up to 14 cm length. Some of these feed rods were sintered at 900°C for 6-10 h under oxygen flow atmosphere. Single crystals were grown using a four-mirror optical floating-zone furnace (CSI System Inc.). Trials were made in which crystals were grown in different atmospheric composition and pressure as follows: flow of air, flow of oxygen, flow of argon, low pressure oxygen (2 atm), high pressure argon-rich (7.5 atm), and high pressure oxygen-rich (10 atm). The crystal growth speed also varied between 2 and 10 mm/hr accompanied by a counter-rotation of the feed and seed rods at 40 rpm.

Na_xCoO_2 was prepared with other Na concentrations (x = 0.5–1.0) using the same basic procedure as described above. However, the sintering temperature was varied with the Na content. For example, the sintering temperature for the x = 1.0 sample was 20°C less than that of x = 0.75 sample. The use of oxygen flow during sintering was found to reduce the number and period of the sintering cycles relative to air flow. However, the effect of oxygen annealing was found to change the magnetic properties of the material, especially at low temperature, as discussed in detail later. Normally, sintering performed on pellets improves the compound formation, but in this case Co_3O_4 impurity phase was observed in sintered pellets due to the slow reaction in the core of the pellet compared to the outer surface area. This may be due to the high densification during sintering which will prevent the oxygen flow to the centre core of the pellet.

Several techniques were used to characterize the grown crystals. Information on the crystal orientation and mosaic was obtained by neutron Laue diffraction. The chemical composition was analysed by electron probe micro-analysis (EPMA). The magnetization of the crystals was measured as a function of temperature and applied field with a superconducting quantum interference device (SQUID) magnetometer (Quantum Design).

3. RESULTS AND DISCUSSION

Compounds with $x < 0.5$ were found to have unreacted Co_3O_4 impurity phase irrespective of the number of sintering cycles or the sintering temperature. Hence, we were unable to achieve single phase material for $x < 0.5$. On the other hand, single phase compound was synthesized for $0.5 \leq x \leq 1.0$ without any detectable Co_3O_4 impurity phase. However, small amounts of CoO impurity phase (<5%) were observed in one or two cases. The amount of impurity was dependent on the sintering condition. Powder XRD studies indicated that the majority phase of the powder and single crystal samples was of a hexagonal structure. The measured a axis parameter for samples with nominally x = 0.75 was found to be a = 2.83 Å virtually independent of preparation conditions, but the c axis parameter was found to vary with respect to the sample preparation. The results for c are given in Table 1. Our value for a for the γ phase hexagonal structure agrees well with that reported elsewhere, but the value of c for the composition x = 0.75 is reported to vary between 10.884 Å and 10.918 Å [20, 10]. The reported variation in c may be due to the difference in the Na/Co ratio, or absorption of moisture, or oxygen non-stochiometry. The variation in c among our samples will be discussed in the following sections. The synthesised powders are very sensitive to moisture, and hence clean and dry storage is crucial. Since Co_3O_4 and CoO impurity phases show up clearly in XRD and magnetization measurements we used these two techniques to search for impurity phases in all our powder and single crystal samples.

During initial experiments we sintered the pressed feed rod used for crystal growth to improve its density and homogeneity, but after sintering the feed rod was found to contain traces of Co_3O_4 impurity phase which developed due to loss of Na during sintering. We believe this evaporation and the consequent decrease in the Na content accounts for the increase in c to 10.913 Å, since there is known to be a systematic increase in c with decreasing x [18]. Surprisingly, crystals grown using the impure feed rod did not contain any impurity. Since Na has a large solubility range in the γ phase ($0.55 \leq x/y \leq 0.74$) in this system, it seems that a small Na loss during sintering is corrected by homogeneous mixing in the molten zone interface. Subsequently we have used green (un-sintered) rods for the crystal growth in order to maintain the Na stoichiometry.

Crystals were grown with both polycrystalline and also single crystal seed rods. One reason for using a polycrystalline seed was to have the same Na composition both in the feed and seed rod. In some cases, Co_3O_4 impurity phase was thought to develop during slow heating of the seed crystal. However, under high pressure growth single crystal seeded runs yielded good quality crystals. The 'necking' technique was employed to improve the grain formation and the parallel platelet crystals were formed after 2–5 cm length of growth. The lower doped ($x \leq 0.65$) crystal growth ended up with small amounts of Co_3O_4 impurity phasedespite having single phase starting powder. This was due to the loss of few percent of Na during crystal growth process. Moreover the size of the single crystal in the boule was very small (~1mm) and very difficult to separate from the grown rod. On the other hand, crystals with $x \geq 0.7$ are single phase and able to cleave large size single crystal from the grown rod. In the later sections we will describe the different conditions used for the growth of $x = 0.75$ crystals in detail. Similar optimum conditions were used for the higher doped crystal growth. Crystals grown under different conditions (named as Crystals A–E) are listed in Table 1. Even from the single-phase green feed rod crystals grown under flowing atmosphere at ambient pressure (Crystal A) or Ar rich atmosphere at high pressure (Crystal C) were found to contain a few percent of Co_3O_4 impurity phase due to Na evaporation or oxygen deficiency during crystal growth. We found that it was very difficult to stabilize the molten zone during atmospheric flow conditions (Crystal A), and hence crystal growth was unsuccessful. Due to the evaporation of Na (which condenses on the inner side of the quartz growth tube) at the time of melting, the molten region ends up being Co_3O_4 rich. Application of 2–3 atm pressure of (mainly) oxygen (Crystal B) during growth was found to reduce the Na evaporation a little. In this case the molten zone was stable for a short while but Co_3O_4 impurity phase was found to be present in the grown boule. A high growth rate (>10 mm/hr) was found to stabilize the molten zone, but it was not helpful to improve the quality or size of the grown crystal. Due to the presence of impurity phase in the grown rod, the separation of the plate-like crystals was very difficult. Application of higher pressure (7.5 atm) to reduce the Na loss, a moderate growth rate (3–5 mm/hr) to improve the crystal quality, and an Ar rich atmosphere (Crystal C — Ar/O_2 ratio = 4:1) enabled us to grow for up to 10 cm length with less Na loss, but a very small amount of Co_3O_4 impurity was still present. However, the c-axis parameter increased to 10.916 Å, which indicates Na loss in the grown crystal.

To investigate the influence of the atmosphere we next applied a gas ratio of O_2/Ar = 4:1 (Crystal D), and used a slightly lower growth rate (3 mm/hr) under the same 7.5 atm pressure. During this growth, Na evaporation was observed to be less compared with the Ar-rich 7.5 atm pressure (Crystal C) and the growth was found to be uniform. The c axis

Table 1. Conditions used to prepare the polycrystalline and single crystal samples of $Na_{0.75}CoO_2$.

Material	Atmosphere	Growth rate	Co_3O_4/ CoO impurity	Na loss	*c* axis parameter value (Å)
Synthesised powder	Flowing O_2 (20 cc/min) (890°C)	—	No	—	10.896
Sintered rod	Flowing O_2 (50 cc/min) (900°C)	—	Yes	Yes	10.913
Crystal A	Flowing O_2 (30 cc/min)	7 mm/hr	Yes	Yes (heavy)	—
Crystal B	2.5 atm pressure, O_2/Ar = 8:1	7 mm/hr	Yes	Yes	—
Crystal C	7.5 atm pressure, O_2/Ar = 1:4	5 mm/hr	Yes	Yes	10.916
Crystal D	7.5 atm pressure, O_2/Ar = 4:1	3 mm/hr	No	Minimum	10.898
Crystal E	10 atm pressure, O_2/Ar = 14:1	4 mm/hr	Little	Yes	10.889

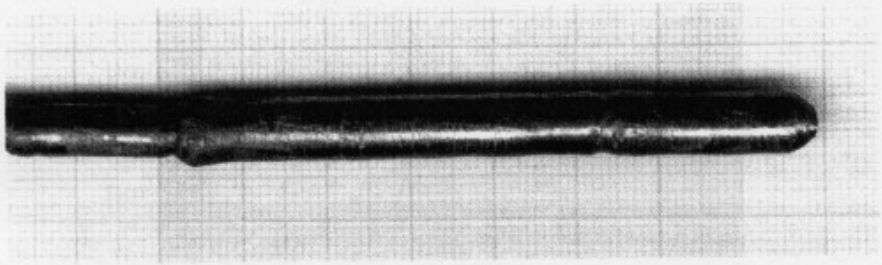

Fig. 1. As-grown seeded single crystal of $Na_{0.75}CoO_2$.

parameter (10.898 Å) was found to be consistent with that of the starting powder. Due to the layer growth mechanism the grown crystal was plate-like in nature along the growth direction, and the large faces were found to be parallel to the crystallographic *ab* plane. The central region of the grown crystal was cleaved and used as a seed for the next run. One such seeded crystal is shown in Fig.1.

Finally, we employed the maximum available oxygen-rich atmosphere (O_2/Ar ratio = 14:1) at a pressure of 10 atm. Several interesting effects were observed. First, we observed that the Na evaporation was slightly higher than during the growth of Crystal D, and secondly, a trace of Co_3O_4 impurity phase was found in the XRD patterns. However, the grown crystal was much more stable when stored in air under ambient conditions than any other of the crystals. The cleaved surface of the crystal was very shiny and stable under atmospheric condition in contrast to crystals grown under low applied pressure whose cleaved crystal surfaces became dull after a couple of hours due to the absorption of moisture. When

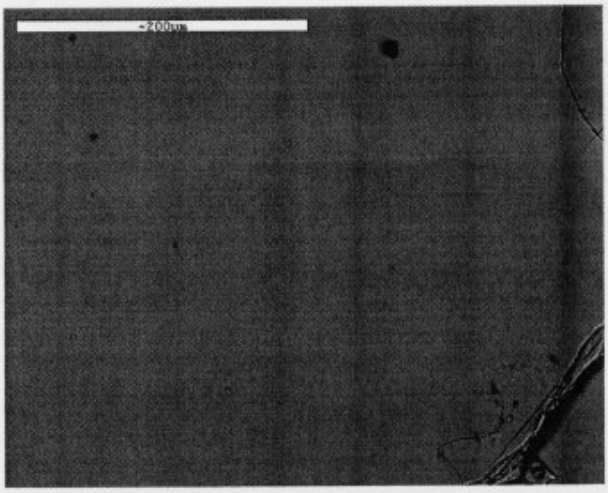

Fig. 2. (**a**) SEM image of $Na_{0.9}CoO_2$ single crystal grown under optimum conditions.

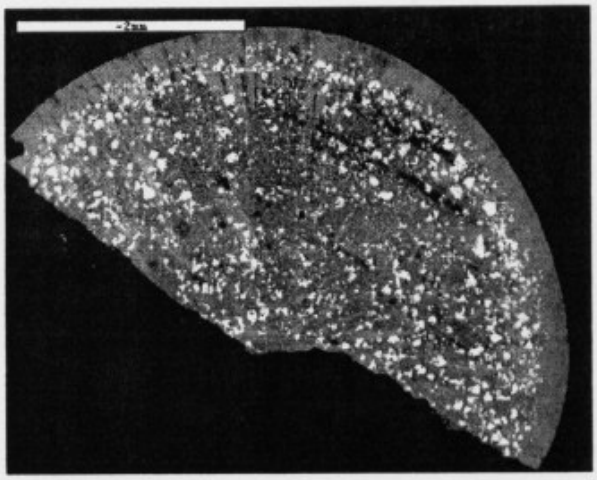

Fig. 2. (**b**) SEM image of cross section view of $Na_{0.65}CoO_2$ single crystal rod. The dark gray particles correspond to Co_3O_4 impurity intergrowths and white particle correspond to Na_2CO_3.

conditions were close to optimum, very clear facets appeared on opposite sides of the crystal rod. These facets were found to be perpendicular to the *c* axis. Crystals grown under low applied pressure (~2–4 atm) did not exhibit facets, but the surface of the crystal rod was observed to be very shiny immediately after growth, but turned white very quickly due to reaction with the atmosphere. Therefore, we assume that a deposition of Na_2O occurred on the outer surface during crystal growth.

The chemical compositions of the grown crystals were checked by electron microscopy combined with EPMA. We first performed compositional analysis at different points along the length of the crystal rod. These measurements did not reveal any variation in the Na/Co ratio along the growth direction. The rest of the measurements were performed on crystal grains cleaved from the top end of crystal rod. These revealed small inclusions of

Co_3O_4 on the surfaces (a few per cent of the area) of the lower doped samples (x = 0.65 and x = 0.7 crystals), but not on any of the higher Na-doped crystals. To illustrate this, a SEM image of the surface of the x = 0.9 crystal used for the EPMA measurement is shown in Fig. 2(a). For comparison, the SEM image for a x = 0.65 crystal is shown in Fig. 2(b). In the latter, the dark gray regions are Co_3O_4 impurity phase, and the white patches correspond to Na rich regions, probably Na_2CO_3 which formed due to the absorption of moisture. The EPMA analysis also revealed that the lower doped crystals (x < 0.75) showed some variation (~10%) in the Na content from point to point on the surface, whereas the crystals with higher doping (x > 0.75) were found to have very little variation in the Na:Co ratio over the surface (~1%). The average Na:Co ratio for the crystals found by EPMA did not always agree closely with the nominal value, but it was neither systematically high nor systematically low. These discrepancies, which in the worst cases were up to 20%, are difficult to understand given that the impurity content was very low. It is possible that the final Na content of the crystal is sensitive to the speed at which the crystal is grown or the growth atmosphere. Another interesting result that we observed was that the maximum Na content in the grown crystal was 0.87 irrespective of the composition of the single phase starting powder ($x \leq 1.0$). For example, we used single phase x = 0.95 starting material for the crystal growth and the grown crystal was found to have x = 0.82. It is very difficult to grow α phase ($0.9 \leq x \leq 1$) single crystal using this technique due to the thermodynamic stability [1]. But recently Takahashi et al., have been grown very thin (~0.1mm) $NaCoO_2$ single crystal by using NaCl flux [27].

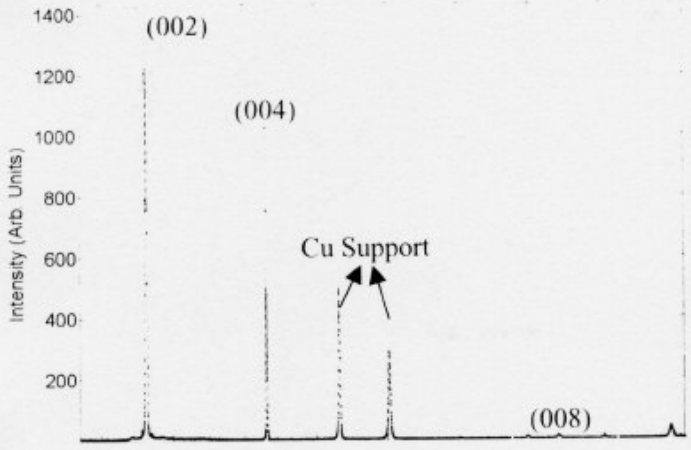

Fig. 3. Single crystal XRD pattern of $Na_{0.75}CoO_2$.

For magnetization and neutron diffraction measurements the crystals were cut into short cylinders perpendicular to the growth direction. The mosaic spread measured by neutron diffraction on a bulk piece of crystal of mass 1.3 g was found to be anisotropic. The in-plane mosaic (i.e. measured by monitoring a Bragg peak while rotating the crystal around the c axis) was found to be 2-3 deg, but the out-of-plane mosaic (measured by rotating the crystal

about an axis in the *ab* plane) was ~10 deg. Smaller crystals cleaved from the main boule had much narrower mosaics. Therefore, we conclude that the bulk crystals grown by the floating-zone method consist of an assembly of plate-like grains stacked together with the grains slightly mis-oriented with respect to one another. The maximum dimension of the cleaved single crystal was 50x7x2 mm^3. The XRD pattern for one such cleaved $Na_{0.75}CoO_2$ crystal oriented for the (00*l*) reflections is shown in Fig. 3. The temperature dependence of the magnetization for the polycrystalline and single crystal samples grown under various conditions is shown in Fig. 4.

The magnetization is quite sensitive to the presence of Co_3O_4 and CoO which exhibit rounded peaks centred near 35 K and 290K, respectively, as shown in the inset to Fig. 4. This impurity was found in all the crystals except crystal D (O_2/Ar ratio = 4:1). The presence of cobalt oxide impurities is most likely due to Na evaporation or oxygen non-stoichiometry.

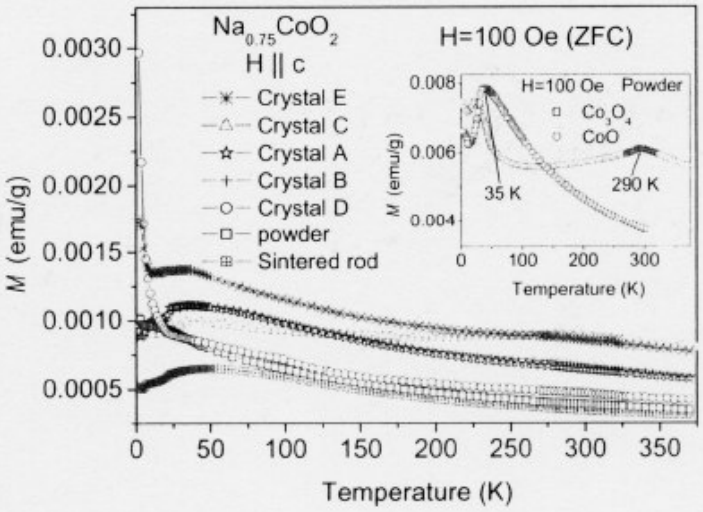

Fig. 4. Temperature dependence of the *dc* magnetization for $Na_{0.75}CoO_2$ polycrystalline and single crystal samples measured in an applied field of 100 Oe. The inset shows the magnetization of Co_3O_4 and CoO powders for reference. These contain peaks due to antiferromagnetic transitions at 35 K and 290 K, respectively.

In general, the use of a high pressure growth atmosphere reduces Na evaporation during growth, but it is also important to choose the correct composition of the atmosphere if the amount of impurity phase is to be a minimum. For example, Crystal E was grown under 10 atm pressure in an O_2 rich atmosphere and had very good crystal quality as described above, but the magnetization curve shows evidence that this crystal contains the Co_3O_4 impurity, in contrast to Crystal D which was grown at a lower pressure. We conclude from this that there is an optimum O_2/Ar ratio near 4:1 for good crystal quality and minimum Co_3O_4 impurity content.

Previously it has been reported that Na_xCoO_2 exhibits a weak ferromagnetic behaviour at low temperatures [32, 33]. This phase has since been observed over a wide range of *x* and at different temperatures [28-31]. However in a diluted Co_3O_4 system, spin-glass behavior has

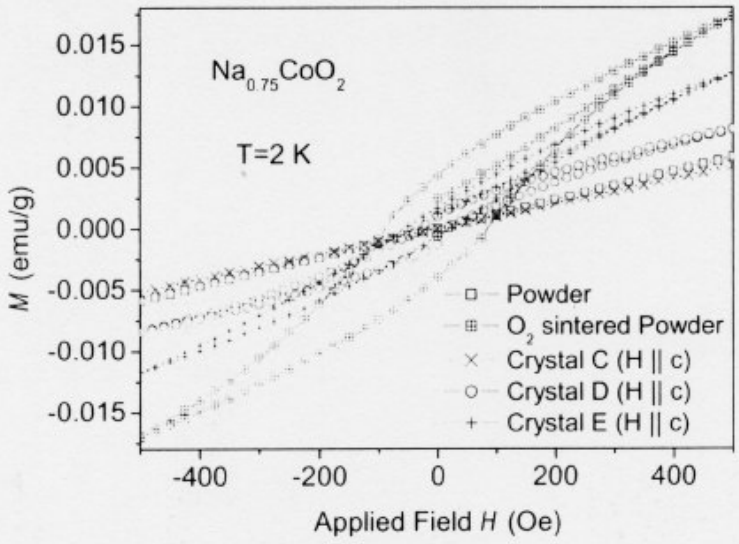

Fig. 5. *Dc* magnetization loop curves for polycrystalline and single crystal samples of $Na_{0.75}CoO_2$ prepared under different conditions.

been noticed below 30 K due to short-range interaction between dipole moments [34]. Our studies have shown that the magnetic irreversibility characteristic of this phase is quite sensitive to the nature and preparation of the sample. To examine this we carried out magnetization measurements as a function of applied field at a fixed temperature of 2 K. The effect of oxygen annealing on the single phase compound was studied by sintering the x = 0.75 single phase powder at ~890°C for 15 h under 20 cc oxygen flow and quenching from 750°C to room temperature. The annealed powder was single phase without any impurity. The field dependence (±500 Oe) of the magnetization for the starting powder, oxygen-annealed powder, Crystal C, Crystal D and Crystal E are shown in Fig. 4. The starting powder is seen to be perfectly paramagnetic with no hysteresis, whereas the oxygen-annealed powder has a very prominent hysteresis loop. Of the crystals, C (grown under pressure in an Ar rich atmosphere) shows no hysteresis, whereas D and E (both grown in O_2 rich atmospheres) both show hysteresis, slightly greater in E than D. Notice also that there is a correspondence between the degree of hysteresis and the magnetization at fixed field above the hysteresis region, e.g. 500 Oe. Extra oxygen might be expected to increase the proportion of Co^{4+}, which carries a spin, relative to non-magnetic Co^{3+}, but this cannot be sufficient to explain the stronger hysteresis effect because samples with lower Na content (and therefore higher Co^{4+}/Co^{3+} ratio) do not show increased magnetic irreversibility at low temperatures [30]. It is possible that the excess oxygen modifies the inter-planar magnetic coupling.

Magnetisation data for the x = 0.95 crystal measured with an applied field of 100 Oe parallel to the *ab* plane and *c* axis is shown in Fig. 6. The magnetization exhibits easy-plane anisotropy. The curves in Fig. 6 show a sharp anomaly at 22 K, corresponding to a magnetic transition that has been widely reported but whose nature is yet to be determined [31, 33]. This anomaly is strongest in the $H \parallel c$ data (both ZFC and FC). We have found that crystals of

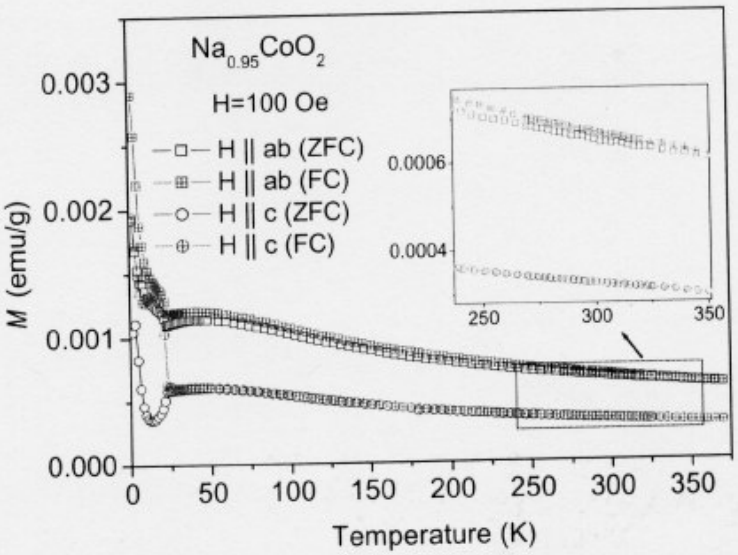

Fig. 6. Temperature dependence of the *dc* magnetization for $Na_{0.95}CoO_2$ single crystal easured in an applied field of 100 Oe along the *ab* and *c* planes. The inset shows the absence of high temperature (320 K) transition in both the planes.

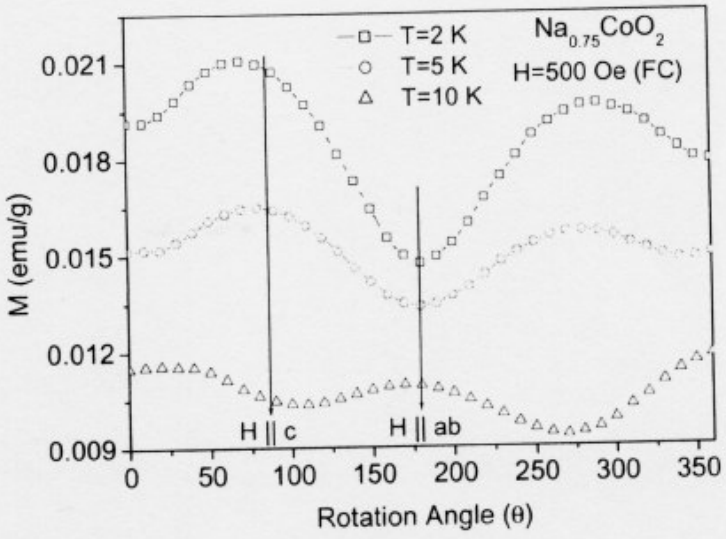

Fig. 7. *Dc* magnetization versus rotation angle of a $Na_{0.75}CoO_2$ single crystal (Crystal D).

lower composition also show a high temperature anomaly near 320 K characterized by a sharp separation of the ZFC and FC magnetization curves [30]. The data in Fig. 6 for $x = 0.95$ do not show this feature for either field orientation. Similar high temperature anomalies have been reported in other bulk properties [23, 35], and these have been attributed to a small structural change associated with Na ordering between the CoO2 layers. The absence of anomaly in the Fig. 6 data could be due to the reduced Na mobility at high Na doping. The this data with $H \parallel ab$ contains a small maximum centred near 40 K which may indicate a trace of Co_3O_4 impurity phase at a level too low to observed by powder XRD (i.e. < 5%).

Finally, we show a measurement in Fig. 7 of the magnetic anisotropy obtained by rotating Crystal D in the magnetometer relative to the applied field direction. What is interesting here is that the sense of the anisotropy switches between 5 K and 10 K. Thus, for $T \leq 5$ K the c axis is the easy direction of magnetization, whereas for $T \geq 10$ K the easy direction is in the ab plane. This indicates that with decreasing temperature below 10 K the spins have an increasing tendency to point along the c axis. However, no such anomaly was observed at low temperature for the higher doped crystals [31].

4. CONCLUSIONS

Our investigations and those of other groups have shown that bulk Na_xCoO_2 ($0.7 \leq x \leq 0.9$) single crystals can be grown by the floating-zone technique with only trace amounts of impurity phases (mainly cobalt oxides). The flux technique may be better to achieve crystals with higher Na content. Further work is needed to improve the mosaic spread of the largest crystals. A number of magnetic features are evident in the bulk magnetization of the crystals. The origins of the 22 K magnetic transition and the anomaly at ~320 K remain open questions. At very low temperatures weak ferromagnetism is observed which is enhanced in samples treated with oxygen. More work is needed to understand these observations.

ACKNOWLEDGMENT

We would like to thank Fred Wondre, Norman Charnley and Shamima Chaudhury for help with the crystal characterization. We are grateful to the Engineering and Physical Sciences Research Council of Great Britain for financial support.

REFERENCES

[1] C. Fouassier, G. Matejka, J-M. Reau and P. Hagenmuller, J. Solid State Chem. 6 (1973) 532.

[2] J. Molenda, C. Delmas and P. Dordor, Solid State Ionics 12 (1989) 473.

[3] K. Mizushima, P.C. Jones, P.J. Wiseman and J.B. Goodenough, Mat. Res. Bull. 15 (1980) 783.

[4] I. Terasaki, Y. Sasago, and K. Uchinokura, Phys. Rev. B 56 (1997) R12685.

[5] K. Takada, H. Sakurai, E. Takayama-Muromachi, F. Izumi, R.A. Dilanian, and T. Sasaki, Nature 422 (2003) 53.

[6] A.T. Boothroyd, R. Coldea, D.A. Tennant, D. Prabhakaran, L.M. Helme, and C.D. Frost, Phys. Rev. Lett. **92** (2004) 197201.

[7] J. Sugiyama, J. H. Brewer, E. J. Ansaldo, B. Hitti, M. Mikami, Y. Mori, and T. Sasaki, Phys. Rev. B 69 (2004) 214423.

[8] B.L. Cushing and J.B. Wiley, J. Solid State chem. 141 (1998) 385.

[9] R. Ishikawa, Y. Ono, Y. Miyazaki and T. Kajitani, Jpn. J. Appl. Phys. 41 (2002) L337.

[10] T. Motohashi, E. Naujalis, R. Ueda, K.Isawa, M. Karppinen, and H. Yamauchi, Appl. Phys. Lett. 79 (2001) 1480.

[11] I. Matsubara, Y. Zhou, T. Takeuchi, R. Funahashi, M. Shikano, N. Murayama, W. Shin and N. Izu, J. Ceram. Soc. Jpn. 111 (2003) 238.

[12] S. Tajima, T. Tani, S. Isobe and K. Koumoto, Mater. Sci. Engg. B86 (2001) 20.

[13] H. Itahara, K. Fujita, J. Sugiyama, K. Nakamura and T. Tani, J. Ceram. Soc. Jpn. 111 (2003) 227.

[14] W.L. Roth, J. Phys. Chem. Solids 25 (1964) 1.

[15] J.R. Singer, Phys. Rev. 104 (1956) 929.

[16] S. Greenwald, Acta Cryst. 6 (1953) 396.

[17] R.J. Balsys and R. L. Davis, Solid State Ionics 93 (1996) 279.

[18] Q. Huang, M.L. Foo, R.A. Pascal Jr., J.W.Lynn, B.H. Toby, Tao He, H.W. Zandbergen, and R.J. Cava, Cond-Mat/0406570 (http://arxiv.org/cond-mat/).

[19] J.D. Jorgensen, M. Avdeev, D.G. Hinks, J.C. Burley and S. Short, Phys. Rev. B 68 (2003) 214517.

[20] J. Sugiyama, H. Itahara, J.H. Brewer, E.J. Ansaldo, T. Motohashi, M. Karppinen and H. Yamauchi, Phys. Rev. B 67 (2003) 214420.

[21] H.W. Zandbergen, M. Foo, Q. Xu, V. Kumar and R.J. Cava, Phys. Rev. B 70 (2004) 24101.

[22] Y.G. Shi, H.C. Yu, C.J. Nie and J.Q. Li, Cond-Mat/0401052. (http://arxiv.org/cond-mat/).

[23] J. L. Gavilano, D. Rau, B. Pedrini, J. Hinderer, H.R. Ott, S. M. Kazakov and J. Karpinski, Phys. Rev. B 69 (2004) 100404.

[24] C. Bernhard, A.V. Boris, N.N. Kovaleva, G. Khaliullin, A. Pimenov, L. Yu, D.P. Chen, C.T. Lin and B. Keimer, Cond-Mat/0403155(http://arxiv.org/cond-mat/).

[25] K. Fujita, T. Mochida and K. Nakamura, Jpn. J. Appl. Phys. 40 (2001) 4644.

[26] M. Mikami, M. Yoshimura, Y.Mori, T. Sasaki, R. Funahashi and I. Matsubara, Jpn. J. Appl. Phys. 41 (2002) L777.

[27] Y. Takahashi, Y. Gotoh and J. Akimoto, J. Solid State Chem. 172 (2003) 22.

[28] R. Jin, B.C. Sales, P. Khalifah, and D. Mandrus, Phys. Rev. Lett. 91 (2003) 217001.

[29] F.C. Chou, J.H. Cho, P.A. Lee, E.T. Abel, K. Matan, and Y.S. Lee, Phys. Rev. Lett. 92 (2004) 157004.
[30] D. Prabhakaran, A.T. Boothroyd, R.Coldea, L.M. Helme and D.A. Tennant, Cond-Mat/0312493 (http://arxiv.org/cond-mat/).
[31] S. P. Bayrakci, C. Bernhard, D.P Chen, B. Keimer, R.K. Kremer, P. Lemmens, C.T. Lin, C. Niedermayer and J. Strempfer, Phys. Rev. B 69 (2004) 100410.
[32] T. Takeuchi, M. Matoba, T. Aharen and M. Itoh, Physica B 312-313 (2002) 719.
[33] T. Motohashi, R. Ueda, E. Naujalis, T. Tojo, I. Terasaki, T. Atake, M. Karppinen, and H. Yamauchi, Phys. Rev. B 67 (2003) 064406.
[34] Y. Hayakawa, S. Kohiki, M. Sato, Y. Sonda, T. Babasaki, H. Deguchi, A. Hidaka, H. Shimooka and S. Takahashi, Physica E 9 (2001) 250.
[35] J. Wooldridge, D. McK. Paul, G. Balakrishnan and M.R. Lees, Cond-Mat/040651 (http://arxiv.org/cond-mat/).